Journal of Experimental Botany, Vol. 58, No. 13, pp. 3695–3710, 2007
doi:10.1093/jxb/erm219 Advance Access publication 10 October, 2007
This paper is available online free of all access charges (see http://jxb.oxfordjournals.org/open_access.html for further details)

Journal of Experimental Botany
www.jxb.oxfordjournals.org

RESEARCH PAPER

Proteomics, pigment composition, and organization of thylakoid membranes in iron-deficient spinach leaves

Anna Maria Timperio[1], Gian Maria D'Amici[1], Csengele Barta[2], Francesco Loreto[2] and Lello Zolla[1,*]

[1] *Dipartimento di Scienze Ambientali, Università 'La Tuscia', L.go dell'Università, 01100 Viterbo, Italy*

[2] *Consiglio Nazionale delle Ricerche, Istituto di Biologia Agroambientale e Forestale, Via Salaria Km. 29 300, 00016 Monterotondo Scalo (Roma), Italy*

Received 29 May 2007; Revised 20 July 2007; Accepted 16 August 2007

Abstract

The changes induced in the photosynthetic apparatus of spinach (*Spinacia oleracea* L.) seedlings exposed to iron deficiency shortly after germination were characterized with two proteomic approaches coupled with chlorophyll and xanthophyll analysis and *in vivo* measurements of photosynthesis. During the first 10 d of iron deficiency the concentrations of chlorophyll *b* and violaxanthin were greatly reduced, but all xanthophylls recovered after 13–17 d of iron deficiency, when both chlorophylls were negatively affected. No new protein was formed in iron-deficient leaves, and no protein disappeared altogether. Photosystem I (PSI) proteins were largely reduced, but the stoichiometry of the antenna composition of PSI was not compromised. On the contrary, PSII proteins were less affected by the stress, but the specific antennae Lhcb4 and Lhcb6, Lhcb2 and its isoform Lhcb1.1 were all reduced, while the concentration of Lhcb3 increased. A strong reduction in thylakoid bending and an altered distribution pattern for the reduced PSI and PSII complexes were observed microscopically in iron-deficient leaves. Supercomplex organization was also affected by the stress. The trimeric organization of Lhcb and the dimerization of Lhca were reduced, while monomerization of Lhcb increased. However, the trimerization of Lhcb was partially recovered after 13–17 d of iron deficiency. In iron-deficient leaves, photosynthesis was strongly inhibited at different light intensities, and a high de-epoxidation status of the xanthophylls was observed, in association with a strong impairment of photochemical efficiency and an increase of heat dissipation as monitored by the non-photochemical quenching of fluorescence. All these negative effects of iron deficiency were attenuated but not fully reversed after again supplying iron to iron-deficient leaves for 7–13 d. These results indicate that iron deficiency has a strong impact on the proteomic structure of spinach photosystems and suggest that, in higher plants, adaptive mechanisms common in lower organisms, which allow rapid changes of the photosystem structure to cope with iron stress, are absent. It is speculated that the observed changes in the monomer–trimer equilibrium of major PSII antennae, which is possibly the result of xanthophyll fluctuations, is a first adaptative adjustment to iron deficiency, and may eventually play a role in light dissipation mechanisms.

Key words: Antenna supercomplexes, BN–PAGE, iron deficiency, pigments, proteomics, RP-HPLC-ESI-MS.

Introduction

Iron deficiency leads to visible morphological and physiological responses in many plants and micro-organisms. In higher plants, the most obvious symptoms of iron deficiency are the development of intercostal chlorosis, principally on young leaves, and morphological changes in roots (Spiller and Terry, 1980).

Many studies have addressed the molecular mechanisms underlying the onset of iron-deficient chlorosis and enzyme activity in chlorotic chloroplasts (Espen *et al*.,

* To whom correspondence should be addressed. E-mail: zolla@unitus.it

Abbreviations: BN–PAGE, blue native–polyacrylamide gel electrophoresis; CAO, chlorophyll *a* oxygenase; DM, *n*-dodecyl-β-D-maltoside; DPS, de-epoxidation status; Lhc, light-harvesting complex; NPQ, non-photochemical quenching; PEG, polyethylene glycol; PSI, photosystem I; PSII, photosystem II; RP-HPLC ESI-MS, reverse phase high-performance liquid chromatography electrospray mass spectrometry.

2000; Nisi and Zocchi, 2000), whereas, apart from a recent study on *Beta vulgaris* (Andaluz *et al*., 2006), there has been little information reported regarding the effect of iron deficiency on thylakoid membranes of higher plants, such as organization of complex components [photosystem I (PSI), PSII, ATP synthase, and cytochrome *b6/f*] and/or super- or subcomplexes.

In contrast to higher plants, the effect of iron deficiency on thylakoid membranes is well documented in lower organisms. In cyanobacteria and *Chlamydomonas*, iron deficiency causes early chlorosis and a reduction in the amount of photosynthetic machinery (Spiller and Terry, 1980; Straus, 1994). In cyanobacteria, iron deficiency results in a degradation of light-harvesting phycobilisomes (Guikema and Sherman, 1983). However, the antenna protein complexes appear to be differentially affected by iron deficiency in these organisms: some specific Lhca1 antennae are drastically reduced, leading to an overall down-regulation of Lhca1, whereas the overall abundance of Lhcb remains fairly constant (Guikema and Sherman, 1983). In iron-deficient cyanobacteria, the PSI:PSII ratio changes from 4:1 to 1:1 (Straus, 1994). PSI appears to be a primary target of iron deficiency, perhaps because of its high iron content (12 Fe per PSI). The adaptation of the multiprotein complexes PSII and PSI to iron starvation is considered to be a sequential process, characterized by the enhanced expression of two major iron-regulated proteins, IdiA (iron deficiency-induced protein A) (Michel and Pistorius, 2004) and IsiA (iron stress-induced protein A) (Bibby *et al*., 2001; Boekema *et al*., 2001). IdiA protects the acceptor side of PSII against oxidative stress under conditions of mild iron limitation in a currently unclear way, whereas prolonged iron deficiency leads to the synthesis of a chlorophyll *a* antenna around PSI trimers consisting of IsiA molecules. IdiA is only bound to dimeric PSII and it is localized by electron micrographs on top of the CP43 subunit facing the cytoplasmic side, in a model derived from the 3D structure of PSII (Loll *et al*., 2005; Lax *et al*., 2007). Eighteen IsiA molecules generate a functional accessory light-harvesting antenna around a PSI trimer, redirecting more light to P700 and forming a PSI–IsiA supercomplex (Bibby *et al*., 2001; Melkozernov *et al*., 2006).

The aims of the present study were to characterize the time course of changes induced in response to iron deficiency in the proteomic profile of thylakoid membranes in a higher plant (*Spinacia oleracea* L.) and to understand whether this affects the photochemistry of photosynthesis. In contrast to previous experiments, plant material that had been deprived of iron from a few days after germination was used in order to minimize the possibility of iron being transferred to leaves from storage organs or the development of other adaptive mechanisms that could lead to higher foliar iron (Morales *et al*., 1998). It was also of interest to determine how plant material that has received no external iron since germination responds to iron supplied in a reconstitution experiment. Two complementary proteomics approaches were used, a two-dimensional electrophoresis [blue native (BN)/SDS–PAGE], and a chromatographic separation, in order to get a complete overview of all photosynthetic components, and in particular of antennae proteins. *In vivo* measurements of photosynthesis and chlorophyll fluorescence parameters were used to understand whether iron-induced changes at the proteomic level, and, in particular, changes in the amount and composition of pigment, are associated with the inhibition of physiological performance under iron deficiency. Combining physiological data with protein and pigment analysis allows a better understanding of the molecular mechanism underlying the adaptation of plants to iron deficiency.

Materials and methods

Plant material

Spinach seeds (*S. oleracea* L.) were disinfected in 1% (v/v) NaClO solution for 10 min followed by thorough washing in deionized water. Seeds were then transferred to a beaker containing 30% (w/v) PEG 8000 for 72 h. Then seeds were washed again in 1% (v/v) NaClO solution and soaked in deionized water for 5 h to rehydrate, with continuous aeration. The seeds were then left to germinate on moist filter paper for 2–3 d. Half of the germinated seeds were sown in moist vermiculite in half-strength Hoagland without iron, and half with 50 μM Fe, and grown for about 5 d (four-leaf stage). After the initial growth period in the seedbed, seedlings were carefully removed from the seedbed, and were thoroughly washed free of any adhering particles under tap water.

The spinach plants were then grown hydroponically in a growth room under a 14 h light period at a light intensity of 260–350 μmol m^{-2} s^{-1}. Temperature was set at 28/20 °C (day/night). The seedlings were transferred to 0.9 dm^3 PVC buckets. Half of the seedlings were grown in half-strength Hoagland nutrient solution (pH 7.7) without iron and under continuous aeration, while the other half were grown in half-strength Hoagland nutrient solution (pH 5.5) with 50 μM Fe and under continuous aeration (Susín *et al*., 1994).

Leaves were harvested after 5, 10, 13, 16, 24, and 30 d of growth in the buckets, and frozen with liquid nitrogen before using them for biochemical measurements.

In the reconstitution experiment, the solution of the iron-deficient plants was replaced after 16 d with the solution used for control plants, and leaves were harvested and frozen after 32 d from the beginning of treatment (16 d after growth under normal iron conditions).

Isolation of intact chloroplasts

Fully developed spinach leaves were used to isolate intact chloroplasts using the method of Nishimura (1976) with minor modifications. Protoplasts were prepared from freshly harvested spinach leaves following the method reported previously (Nishimura *et al*., 1976). The broken protoplasts (0.5 ml) were directly layered on top of 15 ml of a linear sucrose gradient (35–60%, w/w), dissolved in 0.02 M Tricine-NaOH buffer (pH 7.5), and centrifuged at 24 000 rpm for 3 h at 4 °C using a Beckman-Spinco SW 25-3 rotor. Chloroplast numbers were determined as described by Dudley (1958).

Chloroplast structure

The ultrastructural organization of chloroplasts was examined on sections of leaf fragments. Fragments were cut out between leaf ribs and fixed in 1.25% glutaraldehyde in phosphate buffer, pH 7.4, for 1.5–2 h; then specimens were post-fixed in 1% OsO_4 at room temperature for 2 h. The techniques of dehydration, embedding in epoxy resin, thin sectioning, and specimen staining have been previously described (Goodenough and Levine, 1969). Specimens were examined with a JEM-7A electron microscope (Jeol, Japan).

Isolation of thylakoid membranes

For the separation of the thylakoid membrane of chloroplasts from both control and iron-deficient spinach plants, leaves were ground to a powder in liquid nitrogen and subsequently homogenized in an ice-cold 20 mM Tricine, pH 7.8, buffer, containing 0.3 M sucrose and 5.0 mM magnesium chloride (B1 buffer). The homogenization was followed by filtration through one layer of Miracloth (Calbiochem, San Diego, CA, USA) and centrifugation at 4500 *g* for 10 min at 4 °C. The pellet was suspended in B1 buffer and centrifuged again, as above. This second pellet was resuspended in 20 mM Tricine, pH 7.8, buffer, containing 70 mM sucrose and 5.0 mM magnesium chloride (B2 buffer), and centrifuged at 4500 *g* for 10 min. A third pellet was then collected which contained the thylakoid membrane.

BN–PAGE/SDS–PAGE

BN–PAGE of integral thylakoid proteins was performed according to Kügler *et al*. (1997) and Suorsa *et al*. (2004) with the following modifications. Thylakoid membranes were washed with washing buffer [330 mM sorbitol, 50 mM BISTRIS-HCl, pH 7.0, and 250 mg ml^{-1} Pefabloc as a protease inhibitor (Roche, Indianapolis, IN, USA)], collected by centrifugation (3500 *g* for 2 min at 4 °C), and resuspended in 25BTH20G [20% (w/v) glycerol, 25 mM BISTRIS-HCl, pH 7.0, and 250 mg ml^{-1} Pefabloc]. An equal volume of resuspension buffer containing 2% (w/v) *n*-dodecyl β-D-maltoside (DM; Sigma, St Louis, MO, USA) was added under continuous mixing, and the solubilization of membrane protein complexes was allowed to occur for 3 min on ice. Insoluble material was removed by centrifugation at 18 000 *g* for 15 min. The supernatant was mixed with 0.1 vol. of Coomassie blue solution [5% (w/v) Serva blue G, 100 mM BISTRIS-HCl, pH 7.0, 30% (w/v) sucrose, and 500 mM ε-amino-*n*-caproic acid] and loaded onto a 0.75 mm thick 5–12.5% (w/v) acrylamide gradient gel (Hoefer Mighty Small mini-vertical unit; Amersham Biosciences, Uppsala, Sweden). For each sample, the same amount of protein (100 μg) was loaded. Protein concentration was estimated by the Bradford method before the addition of Coomassie blue solution. Electrophoresis was performed at 4 °C by increasing the voltage gradually from 75 V up to 200 V during the 4.5 h run. A ProteanII Bio-Rad (Hercules, CA, USA) electrophoresis system (180×160 mm, 0.75 mm thick) was used for the first dimension applying a constant voltage of 90 V overnight and gradually increasing this value up to 200 V the next day until the run was complete. The first dimension gel images were digitized and the volume of a band was measured using TotalLab version 2.01 (Bio-Rad) on a BN gel. The decrease in protein relative to untreated control after 5, 16, and 24 d of iron deficiency treatment was calculated for each band using the following formula: $(volume_{before}–volume_{after})/volume_{before}$ (Hou *et al*., 2004). Four gel lines were considered for each sample. For separation of proteins in the second dimension, the lanes of the BN gel were excised and incubated in SDS sample buffer containing 5% (v/v) β-mercaptoethanol and 6 M urea for 30 min at room temperature. The lanes were then layered onto 1 mm thick SDS–polyacrylamide gels (Laemmli, 1970) with 15% (w/v) acrylamide and 6 M urea in the separating gel. Proteins were separated overnight at a constant current 10 mA per gel and 13 °C. The proteins were visualized using Blue silver (Candiano *et al*., 2004). Second dimension gel images were digitized and analysed with the PDQuest 7.3 software (Bio-Rad).

Separation of PSI and PSII membrane proteins by sucrose gradient ultracentrifugation and analysis of the contents by HPLC

This technique allows the separation of the antennae proteins of PSI and PSII into distinct chromatographic peaks (Zolla *et al*., 2002, 2003) and makes it possible to analyse them quantitatively. Freshly prepared thylakoid membranes were resuspended at 5 mg ml^{-1} protein in distilled water and solubilized by 1% DM. Purification of PSI was performed according to the method of Croce *et al.* (1998). Briefly, the thylakoid membrane was solubilized by DM to a final concentration of 1%. After stirring for 10 min at 4 °C, the sample was centrifuged for 10 min at 20 000 g, and 6 ml aliquots of the supernatant were loaded onto 0.1–1 M sucrose gradients, containing 5 mM Tricine, pH 7.8, and 0.03% DM. After centrifugation for 42 h at 28 000 rpm in a Model SW28 rotor (Beckman) at 4 °C, five green bands were distinguishable (Caffari *et al*., 2004) that were suitable for direct investigation by reverse phase high-performance liquid chromatography electrospray mass spectrometry (RP-HPLC-ESI-MS).

To resolve the protein components of the antenna systems of PSII and PSI optimally, as isolated complexes by sucrose gradient, an analytical (250×4.6 mm ID) size column was used, packed with the same 5 mm spherical Vydac C-4 stationary phase. The separation of the protein components of the PSII and PSI antenna system was obtained by the following procedure. The Vydac C-4 column was pre-equilibrated with 38% (v/v) aqueous acetonitrile solution containing 0.05% (v/v) trifluoroacetic acid (TFA), and samples were eluted from the column with a gradient of 40–65% acetonitrile in 45 min.

The flow rate was 1.0 ml min^{-1} with the analytical column. The HPLC-ESI-MS experiments were performed by an ion trap Esquire 3000 plus (Bruker Daltonik, Bremen, Germany). Details of the instrumental set-up and tuning are given in Zolla *et al.* (2002). The 1 ml min^{-1} flow through of the analytical column was split post-column, with 50 ml min^{-1} entering the mass spectrometer and 950 ml min^{-1} going to the UV and fluorescence detector. For analysis with pneumatically assisted ESI, an electrospray voltage of 3–4 kV and a nitrogen sheath gas flow were employed. The temperature of the heated capillary was set to 300 °C. Protein mass spectra were recorded by scanning the first quadrupole, the scan range being 500–2000 amu. The quantification of antenna proteins was performed by extracted ion chromatogram (EIC) mass spectrometry. EIC for specific *m/z* signals was selected for quantification of proteins before and after iron stress. For Lhcb6: EIC 846.1; 878.5; 913.5; 951.6; 992.9; 1038; 1087.4; 1141.7 *m/z*. For Lhcb4: EIC 851.7; 878.3; 906.6; 936.8; 969; 1003.6; 1040.7; 1080.7 *m/z*. For Lhcb1.1: 805.5; 832.2; 860.9; 891.6; 924.6; 960.1; 998.4; 1039.9; 1085.1; 1134.4 *m/z*. For Lhcb3: 839.7; 869.7; 901.8; 936.5; 973.9; 1014.4; 1058.4; 1106.4; 1159.2 *m/z*.

Isolation of grana/stroma lamellae

Spinach leaves from control and iron-deficient plants were harvested after 16 d of treatment. The digitonin cleavage and RP-HPLC-ESI-MS were performed according to Timperio *et al*. (2004).

Pigment determination by HPLC

Pigments were extracted from samples by grinding the leaves in liquid nitrogen with degassed 100% acetone at 0–4 °C. On occasion

a small amount of $NaHCO_3$ (0.1 g g^{-1} plant material) was added to the plant material before extraction to ensure no acidification of the extract occurred; however, this had no influence on the carotenoid composition. The pigment extracts were filtered through a 0.2 mm membrane filter and applied immediately to an HPLC column. Pigment composition was determined by HPLC by using a Waters Nova-Pak C18 radial compression column according to Johnson *et al*. (1993). Additionally a Spherisorb ODS-1 column (5 μm particle size, 250×4.6 mm ID) was used based on the method of Gilmore and Yamamoto (1992). To calibrate the method, pigments were first isolated by HPLC. Then isolated fractions were dried under nitrogen and dissolved in the appropriate solvent, and pigment concentrations were determined using the coefficients of extinction indicated in Val *et al*. (1986). The method was calibrated by injecting known amounts of pure pigments, and plotting the peak area (integrator counts) versus quantity of pigment injected. The curve line was made using increasing concentrations of each pure pigment and quantifying each concentration spectrophotometrically. However, considering that the extent of the change is practically the same for all coefficients, results were normalized by dividing by lutein, as reported by De las Rivas *et al*. (1989).

In vivo *and simultaneous measurements of photosynthesis and chlorophyll fluorescence*

Intact plants were used for *in vivo* determination of physiological parameters. A 2 cm^2 circular portion of the leaf was enclosed in a gas-exchange cuvette and illuminated with a KL1500 LCD (Schott, Wiesbaden, Germany) light source using a round fibreglass illuminator (Schott) at a light intensity variable between 0 and 900 μmol photons m^{-2} s^{-1}. The cuvette was kept at constant temperature by water circulating inside the cuvette body, and the leaf temperature was set at 25 °C and measured with a thermocouple appressed to the abaxial leaf side. The leaf disc was exposed to a flow of 500 ml min^{-1} of synthetic air (80% of N_2, 20% of O_2, and 380 ppm of CO_2) adjusted with mass flow controllers (Brooks Instruments BV series 5800, Veenendaal, The Netherlands). The N_2 and O_2 mixture was humidified by bubbling it through water, and the humidity was then reduced by condensing part of it in a water bath set at a temperature lower than the leaf temperature. The relative humidity inside the cuvette was maintained at ~40%, and the vapour pressure difference between the leaf and air was maintained below 20 mbar. The absolute CO_2 concentration in the cuvette was measured with an infrared gas analyser (Gas-hound, Li-Cor, Lincoln, NE, USA), while CO_2 and H_2O exchanges between the leaf and air were measured with a differential infrared gas analyser (Li 6262, Li-Cor). The relationship between photosynthesis and light intensity before and during the iron deficiency treatment was described using a parabolic equation, and best fit lines were generated by the Sigmaplot 2002 software (Systat, Erkrath, Germany). The slopes of regression lines were compared using analysis of covariance (ANCOVA, $P < 0.05$).

Fluorescence was measured with a MiniPAM fluorimeter (Walz, Effeltrich, Germany). The terminal end of a polyfurcated optic fibre was inserted in the round illuminator normal to the leaf plane with the tip reaching the cuvette surface. This fibre was used to supply weak red measuring light and saturating (10 000 μmol m^{-2} s^{-1}) pulses of white light, as well as to detect the emitted leaf fluorescence as described by Loreto *et al.* (1992). The quantum yield of PSII was measured simultaneously with gas-exchange measurements. The fluorescence apparatus described previously was used to measure the quantum yield of PSII in 12 h dark-adapted leaves (F_v/F_m), where F_v is the variable and F_m is the maximal fluorescence. The leaves were then exposed to a light intensity-saturating photosynthesis (700 μmol photons m^{-2} s^{-1}). When photosynthesis was steady, the quantum yield of PSII in the light, $\Delta F/F'_m$ (Genty *et al*., 1989), was measured (data not shown). The photochemical and non-photochemical quenching of fluorescence (qP and qN, respectively) were calculated according to the protocol described by Van Kooten and Snel (1990), and the fluorescence nomenclature reported in that paper was followed. To calculate correctly the basal fluorescence with all reaction centres open (F'_o), a parameter required in the calculation of fluorescence quenchings, a flash of far-red light was supplied using the PAM 101 source immediately after darkening the leaf. The non-photochemical quenching of fluorescence was also calculated according to Bilger and Bjorkman (1994) to yield the light dissipated non-radiatively (NPQ). This parameter is calculated on the basis of the ratio between maximal fluorescence in the dark and in the light [$NPQ=(F_m/F'_m)-1$].

Every measurement was repeated on at least four different leaves of different plants. Statistical separation between means was carried out with a Tukey's test, and differences significant at a $P < 0.01$ or < 0.05 are shown by *** and **, respectively.

Results

Pigment analysis

Chloroplasts from plants germinated and grown in iron-deficient conditions were analysed for their biochemical composition, structure, and function. Plants grown in the absence of iron for 16 d showed a reduction in the total number of chloroplasts (<30%) with respect to controls. Iron-deficient chloroplasts also contained 40% less total protein and 62% less chlorophyll than chloroplasts of control leaves (data not shown). Consequently the protein/chlorophyll ratio increased, indicating that each chlorophyll-binding protein contained fewer chlorophyll molecules than in normal conditions.

The time course of the iron deficiency-driven changes of total chlorophyll, and chlorophyll *a* and *b*, was determined spectrophotometrically (Fig. 1A) and by HPLC (Fig. 1B), in order to get rapid chlorophyll quantification by the first method and more laborious but precise chlorophyll *a* and *b* determinations by HPLC. The two methods yielded comparable data. During the first 13 d of iron deficiency, chlorophyll *b* was more negatively affected than chlorophyll *a*, and the ratio between chlorophyll *a* and *b* consequently increased (both insets of Fig. 1). Between 13 d and 16 d of iron deficiency, both chlorophyll *a* and *b* were negatively affected. Interestingly, in the iron reconstitution experiment, a re-synthesis of both chlorophylls was recorded, but the total amount of chlorophyll remained lower than that detected in control plants, at least after 9 d.

During the first 10 d of iron deficiency a significant decrease of violaxanthin was observed, accompanied by an increase in both antheraxantin and zeaxanthin (Fig. 2). The change in violaxanthin concentration occurred with the same time course observed for the decrease in chlorophyll *b* (see Fig. 1). However, after 13–16 d of iron deficiency, when both chlorophyll *a* and *b* decreased (Fig. 1), violaxanthin recovered from its minimum, as did zeaxanthin and anteraxanthin. After 20 d, while

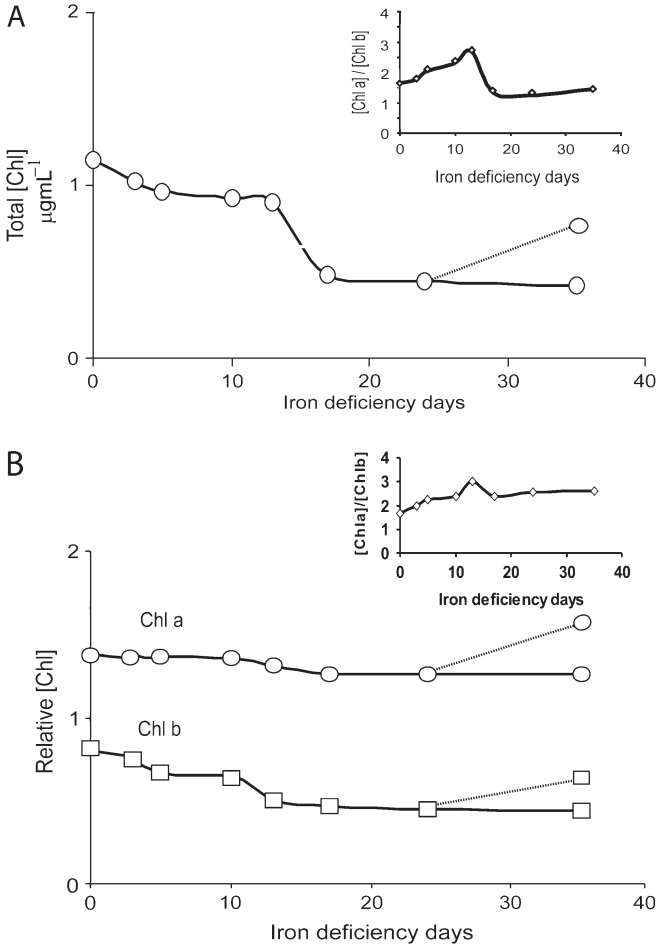

Fig. 1. Time course of the total leaf chlorophyll concentrations measured in chloroplast membranes of iron-deficient spinach plants by both spectrophotometric (A) and HPLC (B) methods. In (A), the total chlorophyll concentration was estimated at 652 nm using solutions with the same number of chloroplasts. The inset shows the time course of the chlorophyll *a*/chlorophyll *b* ratio determined by the absorbance of the pigments at the respective wavelengths. In (B), the concentrations of chlorophyll *b* (Chl b, open squares) and chlorophyll *a* (Chl a, open circles) were measured by the area underlying the corresponding HPLC peaks. The inset shows the time course of the chlorophyll *a*/chlorophyll *b* ratio obtained from the relative peak areas. In (B), the absolute abundances of chlorophyll *b* and *a* were scaled by a normalizing factor which was obtained by comparing in the different extractions the absolute abundance of lutein, a pigment whose concentration remains unchanged during iron deficiency. The dotted line shows the total chlorophyll determined after restoring iron supply after 24 d.

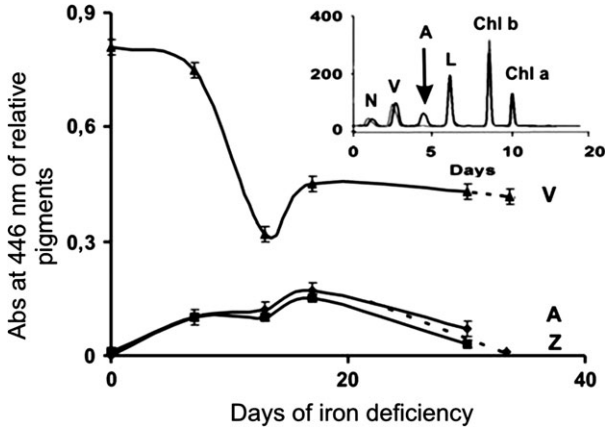

Fig. 2. Time course of leaf photosynthetic pigment concentrations determined by HPLC analysis on thylakoid membrane of spinach iron-deficient plants: filled triangles, violaxanthin (V); filled diamonds, antheroxanthin (A); and filled squares, zeaxanthin (Z). The dotted line shows the violaxanthin and antheraxanthin concentrations determined in iron-deficient plants supplied with iron, starting after 24 d of iron deficency. The inset compares the HPLC chromatograms of pigments, including also lutein (L), neoxanthin (N), and chlorophylls, extracted after 10 d of recovery, from plants in which iron nutrition was restored (grey line) or maintained under iron deficiency (black line). The arrow indicates the anteraxanthin peak.

violaxanthin remained constant, both zeaxanthin and anteraxanthin decreased again (Fig. 2).

When iron was supplied to iron-deficient plants, the levels of lutein, violaxanthin, and neoxanthin did not change, while both antheraxanthin and zeaxanthin disappeared (Fig. 2 and Fig. 2 inset).

Proteomic analysis

One of the most obvious characteristics of iron-deficient leaves is chlorosis, but it has never been clarified whether specific proteins are affected by iron deficiency in higher plants. Previous studies have shown the limitations of proteomic analysis by electrophoresis, especially for differentiating between antenna isoforms (Ciambella *et al*., 2005). A proteomic analysis of the four main complexes present in the thylakoid membranes was therefore performed using both electrophoretic and chromatographic protein separations.

It has previously been documented that the proteome of the photosynthetic apparatus of higher plants can be successfully analysed in thylakoids without previous fractionation (Aro *et al*., 2005; Ciambella *et al*., 2005), and for this reason the investigation was started with two-dimensional BN–PAGE/SDS–PAGE of thylakoid membranes.

First dimension electrophoretic dimension

BN–PAGE separation of thylakoid proteins from stressed and unstressed plants was compared and analysed (Fig. 3A). Since the apparent molecular masses of the protein complexes in the first dimension native PAGE corresponded to the predicted molecular masses of all compounds, each complex can be recognized by its molecular mass as reported in the right panel of Fig. 3A (Ciambella *et al*., 2005). To quantify the volume of each band, the image analysis software TotalLab vers. 2.01 (Bio-Rad) was used. The semi-quantitative decrease in protein relative to day 0 (control) was calculated 5, 10, 16, and 24 d after the beginning of iron deficiency (Fig. 3B) Data shown refer to the average of three different experiments. In iron-deficient leaves, the bands attributed to two supercomplexes having the apparent molecular masses of

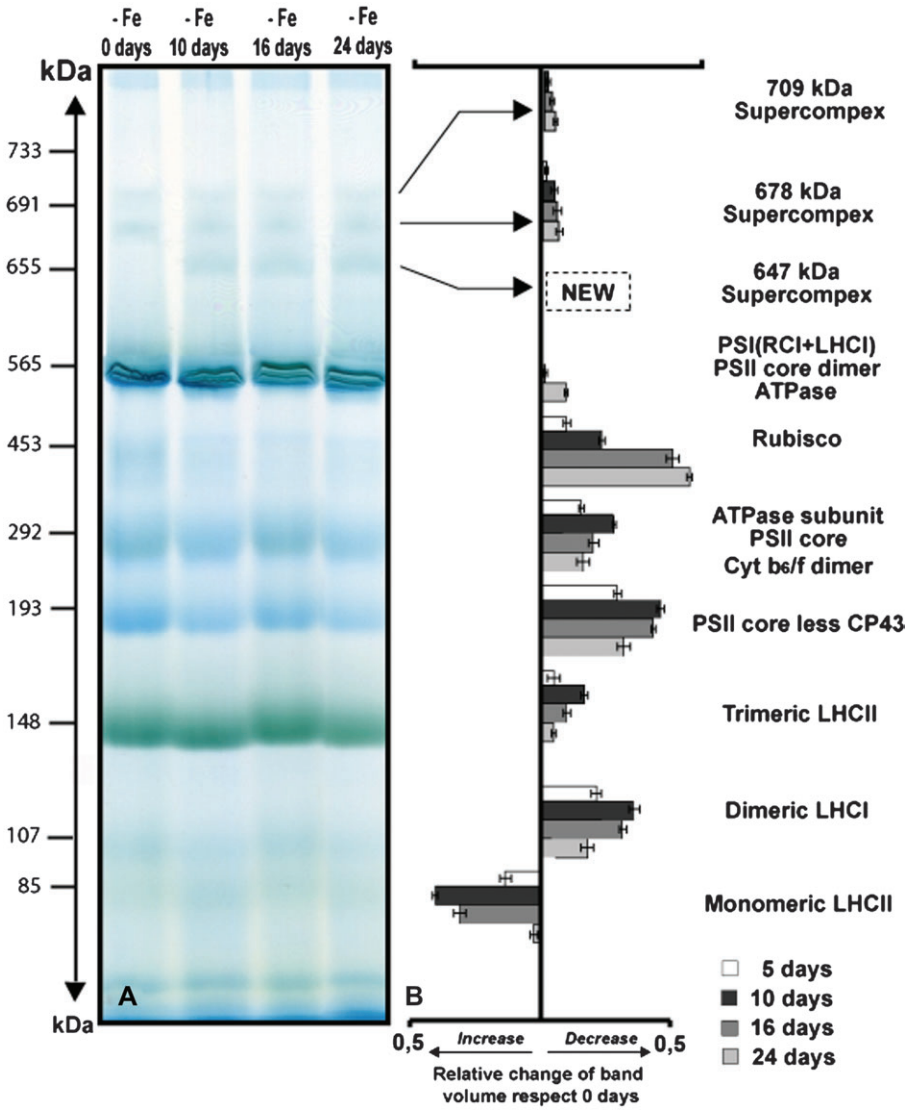

Fig. 3. Comparison of the blue native–PAGE profile of thylakoid membrane protein complexes from plants after 0, 10, 16, and 24 d of iron deficiency (A). Each strip of (A) was loaded with the same amount of protein (100 μg), as estimated by the Bradford method. In (B), the relative decrease of band volume with respect to 0 d of iron deficiency was calculated for each protein complex measured after 5, 10, 16, and 24 d of iron deficiency. Four gel lines for each sample were considered for these calculations.

709 kDa and 678 kDa, and containing both PSI and PSII proteins (Aro *et al*., 2005; Ciambella *et al*., 2005), showed a reduction in colour intensity over the time course (Fig. 3A, upper part), while a new band at a lower molecular mass of 647 kDa, containing both PSI and PSII proteins (see later), appeared after 10 d of stress. This could be an indication that the super organization of thylakoid membranes was strongly compromised and a new re-arrangement took place in iron-deficient chloroplasts. A significant decrease in Rubisco (453 kDa) was observed with prolonged iron deficiency. There was also a reduction in two close running Coomassie-stained bands (at 292 kDa and 193 kDa) in iron-deficient leaves. These two bands represent the ATP synthase subunit, the dimeric cytochrome *b6/f* complex, the monomeric PSII core complex (292 kDa), and the monomeric PSII core complex without CP43 (193 kDa). The two bands at about 148 kDa and 85 kDa, representing the trimeric and monomeric forms, respectively, of the light-harvesting complex of PSII (Ciambella *et al*., 2005; Granvogl *et al*., 2006), showed large and opposing changes in iron-deficient leaves. The dimeric form of antenna proteins at about 107 kDa was also greatly reduced in conditions of sustained iron deficiency. Interestingly, however, the decrease in the amount of units organized into trimers and dimers, and the increase in the monomeric form, peaked after only 10 d of iron deficiency and then re-aggregation tended to revert to the levels of control leaves. Thus, in both photosystems, a sequence of events was observed, with antennae aggregation rapidly

compromised by iron deficiency, and then recovering when both chlorophylls *a* and *b* were negatively affected and the de-epoxidation status of the xanthophylls changed.

Second dimension electrophoretic dimension

All protein complexes separated by the first dimension native electrophoresis were directly transferred and analysed in the second denaturing SDS–PAGE where protein subunits of the thylakoid membranes were distributed by their distinct molecular masses, and proteins were recognized by separated vertical lines in the 2D gel (Fig. 4A). The PDQuest (Bio-Rad) analysis was used to identify proteins that increased or decreased significantly as a result of iron deficiency (Fig. 4B). An almost regular distribution of proteins deriving from complexes and supercomplexes was apparent. Visible spots of membrane proteins were cut out from the SDS–polyacrylamide gel, digested with trypsin, and analysed either by matrix-assisted laser desorption ionization-time of flight (MALDI-TOF) or by internal peptide sequencing, using mainly RP-HPLC-ESI-MS/MS, as previously reported (Ciambella

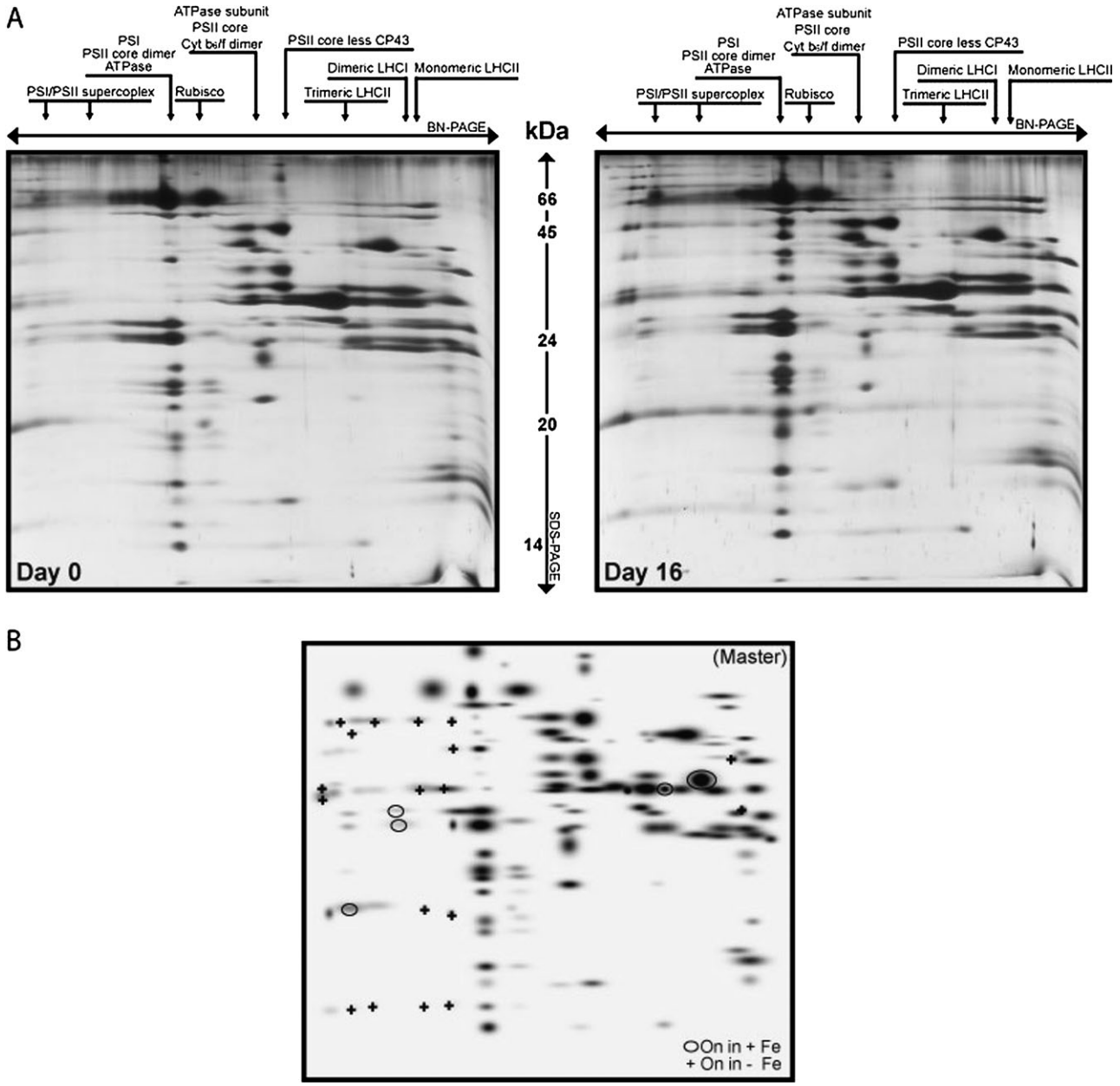

Fig. 4. Two-dimensional BN–PAGE/SDS–PAGE maps of thylakoid membrane proteins extracted after 0 d and 16 d of iron deficiency in spinach leaves (A). In (B), the master map of thylakoid membrane differences was created by comparison of the maps of (A) after 0 d and 16 d of iron deficiency. This analysis was performed by PDQuest software. In (B), symbols refer to the type of qualitative variation: open circles, present only in the leaves after 0 d of iron deficiency; +, present only in leaves after 16 d of iron deficiency.

et al., 2005). Analysis of the data confirms (data not shown) that the first three lanes on the left contain supercomplexes of PSI and PSII, the fourth lane the PSI, dimeric PSII core proteins, and some of the ATP synthase proteins, the fifth lane contains the Rubisco components and the monomeric core proteins from PSI, and the sixth lane contains a mixture of ATP synthase complex, cytochrome b_6/f dimer, and monomeric core of PSII. Finally the seventh lane contains the monomeric core of PSII without CP43. Regarding the PSII antenna proteins, they were detected both in supercomplexes and in the eighth and tenth lanes, corresponding to the trimeric and monomeric state of PSII light-harvesting proteins.

It can be seen that significant changes appeared only in the lines corresponding to supercomplexes and in the antennae regions, confirming their different distributions in iron-deficient leaves (see circles in Fig. 4B). This analysis also revealed that the main constituents of both PSI and PSII were present in normal proportions in iron-deficient leaves. Thus, there was no reduction in specific components of the photosystems. Rather, all components of the photosystems decreased in concert, maintaining a constant stoichiometry, during iron deficiency.

Chromatographic separation of thylakoid membranes

In order to investigate further the differences in antenna composition inside complexes, a liquid chromatographic separation was performed, since previous investigations (Gomez *et al*., 2002; Zolla *et al*., 2002, 2007) revealed that by this method a better qualitative and quantitative antenna determination can be performed than by two-dimensional electrophoresis. The five green fractions obtained by loading thylakoid membranes onto a sucrose gradient were analysed for their content by RP-HPLC-ESI-MS. The band (B1) containing monomeric PSII antennae (Caffari *et al*., 2004) was more abundant in iron-deficient leaves than in controls (Fig. 5A). A second band (B2) corresponding to Lhcb trimeric aggregation (Caffari *et al*., 2004) was also fainter in iron-deficient leaves than in controls. This confirms indications obtained by two-dimensional BN electrophoresis that antenna trimerization was reduced during iron deficiency. In iron-deficient plants, a band (B3) containing subcomplexes of Lhcb–Lhcb4–Lhcb6 (Caffari *et al*., 2004) and a band (B5) that contains PSI–Lhca were also strongly reduced, as shown by the lighter colour intensity (Fig. 5A). Band 4, due to the high hydrophobicity of the PSII core proteins, could not be analysed quantitatively, as it requires different experimental conditions to be analysed by HPLC (Gomez *et al*., 2002; Huber *et al*., 2004). Each band, except B4, was collected by a syringe and components were analysed by HPLC. Figure 5B shows a chromatogram of B1 and B2 together which represent the total PSII antenna. Protein identification was performed by comparison of the measured molecular masses with those deduced from the DNA sequence (Zolla *et al*., 2004; Whitelegge *et al*., 2006).

All antenna proteins were affected by iron deficiency. Quantification of antenna proteins was performed by EIC mass spectrometry by using specific *m/z* signals. The minor light-harvesting complex II antenna proteins were the most depleted. This reduction was especially evident for Lhcb6 (75%) and Lhcb4 (44%), while Lhcb1.1 decreased by only 10%. This was also confirmed by HPLC of the B3 fraction, which contained the Lhcb–Lhcb4–Lhcb6 subcomplex (Caffari *et al*., 2004) (Fig. 5C). Analysis of Lhcb4 and Lhcb6 subcomplexes, identified by mass spectrometry (data not shown), showed a dramatic reduction of these fractions with respect to the major antenna proteins. Interestingly, a general increase in Lhcb3 (~20%) was observed in iron-deficient leaves, especially in the subcomplexes Lhcb–Lhcb4–Lhcb6 (see Fig. 5C). Lastly, the chromatographic profile of B5 (Fig. 5D) showed that, in iron-deficient plants, the peaks corresponding to PSI antennae of Lhca were smaller, while a significantly higher presence of Lhcb1 and Lhcb2 of PSII (peaks released after 25 min or more) was observed. This suggests that PSI lamellae of iron-deficient plants are rich in PSII components and that the presence of these components becomes evident when the functional organization of PSI is damaged.

In order to collect more information on the last point, grana and stroma were separated from the thylakoids of control and iron-deficient leaves by digitonin, as previously demonstrated (Timperio *et al*., 2004). The protein composition of each subfraction and the amount of PSI and PSII in each subfraction was then determined again by HPLC on control and 16 d iron-deficient leaves. Grana lamellae from both control and stressed plants contained prevalently PSII antenna proteins; however, stroma lamellae from stressed plants contained a large amount of PSII Lhcb1, whereas the control did not, indicating an aberrant distribution of PSI and PSII in stroma lamellae of iron-deficient leaves (Fig. 6A). Electron micrographs of chloroplasts from mesophyll cells of 16 d iron-deficient leaves revealed plastids with few photosynthetic lamellae and with some rudimentary grana, displaying the classical features of thylakoid disorganization induced by iron deprivation (Thoiron *et al*., 1997) (Fig. 6B).

In vivo *analysis of photosynthesis and fluorescence*

Physiological measurements were taken before iron removal and again after the pigment composition changed dramatically as a consequence of iron deficiency (13–18 d after beginning the treatment, see Figs 1 and 2), and after a 7 d recovery from iron deficiency. Photosynthesis in leaves deprived of iron for 13–18 d did not increase at light intensities >200 μmol m^{-2} s^{-1} (Fig. 7). The rate of photosynthesis responded linearly to increasing light

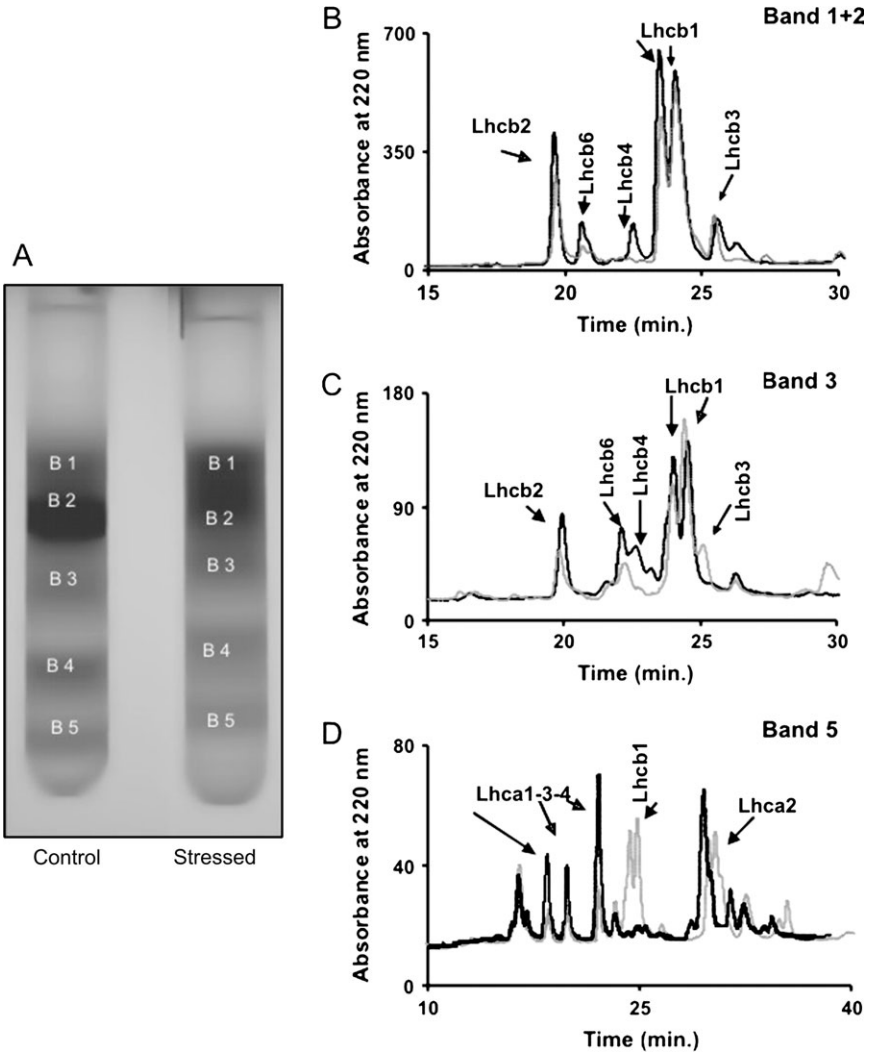

Fig. 5. Separation on a sucrose gradient of thylakoid subcomplexes into five different fractions (B1–B5) in control (0 d of iron deficiency) and stressed (16 d of iron deficiency) spinach leaves (A). In (B–D), the HPLC analysis of each thylakoid subcomplex in leaves after 0 d (black lines) or 16 d (grey lines) of iron deficiency is shown. The peaks corresponding to the main subcomplexes identified by this analysis are shown with arrows.

intensity for light intensities ranging between 0 and 150 μmol m^{-2} s^{-1}. In this range a significant reduction in the apparent quantum yield (the ratio between photosynthesis and incident light intensity) was measured in iron-deficient leaves. The quantum yield was 0.27, 0.17, and 0.21 before iron removal, after 13–18 d of iron deficiency, and after a 7 d recovery from iron deficiency, respectively. These differences were statistically highly significant (Tukey's test, P <0.01).

Reduced efficiency of light capture by the photochemical apparatus of iron-deficient plants was also suggested by the analysis of chlorophyll fluorescence. In dark-adapted leaves, the ratio between variable and maximal fluorescence (F_v/F_m), a sensitive indicator of the efficiency of PSII, was decreased on average by 40% in leaves subjected to 13–18 d of iron deficiency with respect to the values observed in the same leaves before iron removal (Fig. 8). In illuminated leaves, the non-photochemical quenching, indicating increasing energy dissipation, doubled after 13–18 d of iron deficiency, while the photochemical quenching, indicative of the electron transport rate driving photosynthesis and photorespiration, was significantly reduced at the onset of iron deficiency. All fluorescence parameters recovered very rapidly during the iron reconstitution experiment (Fig. 8). After 7 d growth with reconstituted iron, the photochemical quenching was not statistically different from that measured before iron deficiency. The F_v/F_m index and the non-photochemical indices also recovered but were still significantly different from control leaves, indicating the persistence of mechanisms of energy dissipation activated by iron deficiency.

The de-epoxidation status of xanthophylls (the amount of antheraxanthin+zeaxanthin divided by the sum of antheraxanthin+zeaxanthin+violaxanthin=DPS) increased with the period of iron deficiency, and this change was

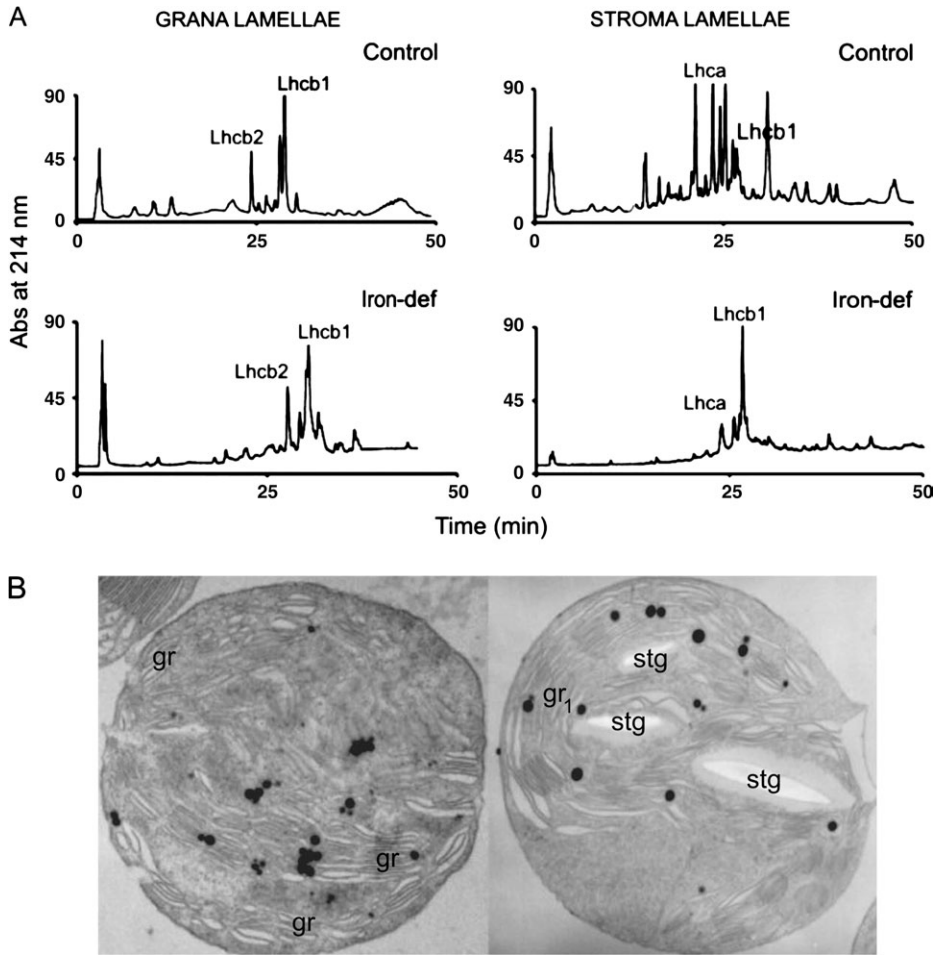

Fig. 6. In (A), chromatographic fingerprints of the antenna proteins contained in the grana (left) and in the stroma lamellae (right) from leaves after 0 d (upper figures) or 16 d of iron deficiency (lower figures) are shown. In (B), the chloroplast structure of the fifth leaf pairs of spinach after 0 d (left) and 16 d of iron deficiency (right) is shown by electron microscopy (magnification ×42 000). Gr, grana; gr1, rudimentary grana; stg, starch granule.

associated with the increasing amount of non-photochemical quenching. This association was also found in leaves recovering from iron deficiency (Fig. 9). However, the DPS was maximum (=0.45) at day 13, i.e. when the amount of violaxanthin was observed to fall to its minimum level (see Fig. 2). In the following days, violaxanthin and the DPS partially recovered (a DPS of 0.39 was observed at day 18), but these changes were not associated with changes (reductions) in non-photochemical quenching (Fig. 9).

Discussion

Pigment analysis suggests the activation of a mechanism of adaptation to iron deficiency to scavenge excess light

In plants grown from germination in the absence of iron, a clear association between chlorophyll *b* and violaxanthin depletion was observed during the first 10 d of iron deficiency. However, the recovery of xanthophylls after 13 d of iron deficiency, when both chlorophyll *a* and *b* were negatively affected by the treatment, was unexpected and is interpreted as evidence of the activation of mechanisms of adaptation to iron deficiency. The increase of xanthophylls may help leaves cope with excess light that cannot be used efficiently by photosynthesis (especially when chlorophylls are depleted) and that may be scavenged non-radiatively through the violaxanthin–zeaxanthin de-epoxidation cycle (Demmig *et al*., 1987; Brugnoli *et al*., 1998). However, *in vivo* analysis of photosynthesis photochemical and non-photochemical use of the light energy, as discussed below, does not specifically confirm that xanthophyll resilience may contribute to decrease the non-radiative dissipation of light in iron-deficient leaves.

Proteomic analysis confirms also in higher plants high sensitivity of PSI to iron deficiency and shows different sensitivity of antenna proteins to the stress

Iron deficiency drastically reduced the amount of protein from both photosystems and also from cytochrome *b6/f*

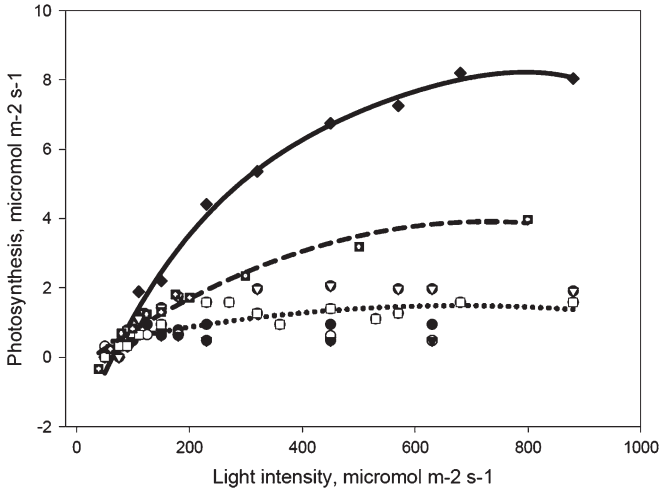

Fig. 7. Photosynthesis response to incident light intensity in a leaf before iron deficiency (day 0 of the treatment, filled diamonds) as compared with photosynthesis of leaves after 13 (filled circles), 14 (open circles), 15 (filled triangles), 16 (open triangles), and 18 (open squares) days of iron-deficient nutrition, and after 7 (crossed squares) days of iron re-supply. Best fit lines to the response before iron deficiency (solid line), after 13–18 d of iron deficiency (dotted lines), and after iron re-supply (dashed line) were generated by the Sigmaplot 2002 software (Systat, Erkrath, Germany). The slopes of the best fit lines are all significantly different (ANCOVA, $P < 0.05$).

and the ATP synthase complex. Within each photosystem, all core components were present, which indicates that iron deficiency does not inhibit altogether the synthesis of a specific core protein. However, separation of complexes on a sucrose gradient showed that the entire PSI complex was the most sensitive complex, with reduction of both the light-harvesting and core complex proteins, as previously observed (Nishio *et al*., 1985). Similar observations were made with prokaryotic organisms. In *Acaryochloris* cells grown in an iron-deficient medium, the level of PSI was also found to decrease compared with that of PSII (Chen *et al*., 2005). In these cells, the iron-deficient medium induced an up-regulation of the *pcbC* gene in comparison with the *pcbA* gene (Chen *et al*., 2005).

In cyanobacteria, adaptation to iron starvation is characterized by the enhanced expression of two major iron-regulated proteins, IdiA (Michel and Pistorius, 2004) and IsiA (Bibby *et al*., 2001). However, no new protein was observed in spinach leaves exposed to iron deficiency. This was also somewhat expected since no IdiA homologue proteins were identified in *Arabidopsis thaliana* (http://www.arabidopsis.org) and these proteins may be absent in higher plants.

The total amount of antenna proteins was significantly reduced in both photosystems of spinach leaves. In cyanobacteria, the most obvious alterations under iron starvation are the reduction of phycobilisomes and chlorophyll-containing proteins (Straus, 1994), in part due to phycobilisome protein degradation and in part to a reduction of *de novo* protein synthesis (Sandstrom *et al*., 2002). In spinach, however, the stoichiometry of the antenna composition of PSI was not compromised. On the contrary, specific antennae of PSII were strongly reduced, e.g. Lhcb4 and Lhcb6, Lhcb2, and the isoform of Lhcb1 (Lhcb1.1), while Lhcb3 increased. In *Chlamydomonas*, an opposite effect was observed, as specific components of Lhca were strongly reduced at the onset of iron deficiency, whereas Lhcb abundance remained fairly constant (Hippler *et al*., 2001).

In higher plants, the antenna sizes are controlled by the biosynthesis of chlorophyll *b* (Tanaka *et al*., 2001). A close relationship between chlorophyll *b* synthesis and *cab* gene expression was also found by Pattanayak *et al*. (2005). In particular, chlorophyll *a* oxygenase (CAO)-deficient mutants, which form low levels of chlorophyll *b*, showed reduced amounts of PSII antennae by electrophoresis (Tanaka and Tanaka, 2005). This is in agreement with the present results obtained by chromatographic separation and mass spectrometry, i.e. with a better separation of the antennae and their unambiguous quantification.

Proteomic analysis reveals reduction of large compexes and supercomplexes, and aggregation of proteins in small complexes in iron-deficient leaves

The observed decrease of Lhcb4 and Lhcb6 may specifically and negatively influence the formation of supercomplexes and/or megacomplexes. In fact, Lhcb4 is located in the interior of the supercomplex, and Lhcb6 is essential for the formation of type I and type III megacomplexes (Dekker and Boekema, 2005). Similar to results obtained in cyanobacteria (Pakrasi *et al*., 1985), BN electrophoresis revealed that large complexes and supercomplexes are also less abundant in iron-deficient leaves in spinach, indicating that aggregation of small complexes into higher order structures is also affected by this stress. The responses of *Chlamydomonas* to iron deficiency also include remodelling of the antenna complexes (Naumann *et al*., 2005), disconnection of the Lhca antenna from PSI, and the establishment of a new steady state, with decreased stoichiometry of electron transfer complexes (Moseley *et al*., 2002). However, the strongly compromised superorganization of the photosynthetic apparatus observed in spinach iron-deficient leaves may not be completely explained by the reduction in the total number of antennae and by the specific loss of minor PSII antennae. The present two-dimensional BN–SDS results show that the decrease in Lhcb trimers, the increase in the monomeric form of the same complex, and the decrease in Lhca dimerization occurred after 10 d of iron deficiency and tended to be reversed as iron deficiency continued. This suggests that the decrease of chlorophyll *b*, occurring with the same time course observed for the changes in the anteannae in iron-deficient leaves, induces monomerization of antennae. Since in higher plants, Lhcbs are able to bind both chlorophyll *a* and chlorophyll *b*

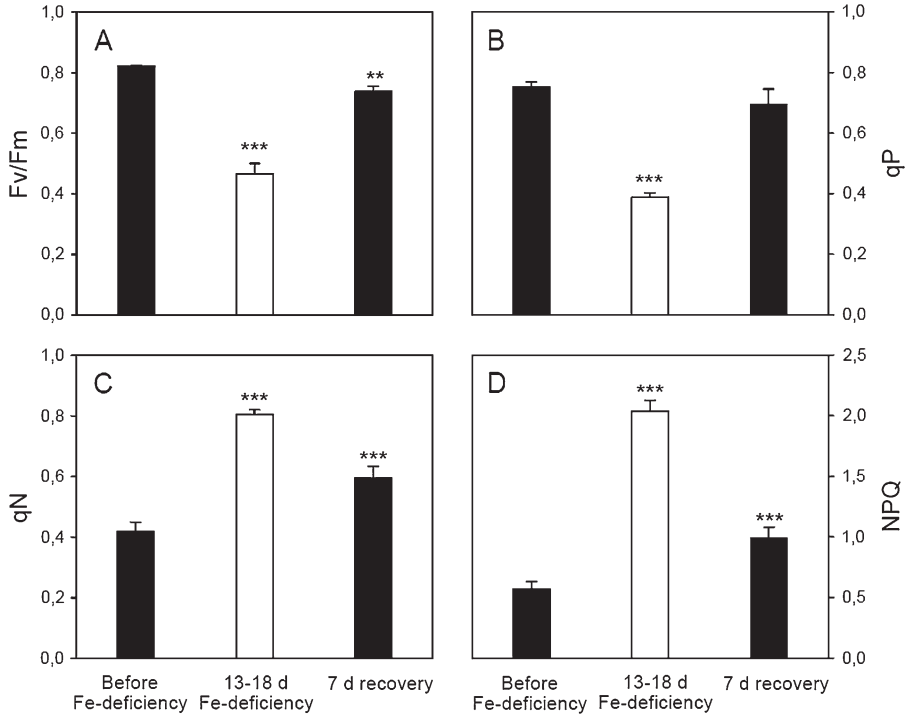

Fig. 8. Fluorescence parameters before iron deficiency, after 13–18 d of iron deficiency, and after a 7 d recovery from iron deficiency. The maximal quantum yield of PSII (F_v/F_m; A), the photochemical quenching (qP; B), and the non-photochemical quenching calculated according to the nomenclature of van Kooten and Snel (1990) (qN; C) and according to the Stern–Volmer equation (NPQ; D) are shown. Means and standard errors (n=5) are shown. Means were separated statistically by ANOVA, and statistical differences were assessed by Tukey's test. Means different at P <0.01 and P <0.05 are shown by *** and **, respectively.

interchangeably both *in vitro* (Bassi *et al*., 1999; Xu *et al*., 2001) and *in vivo* (Polle *et al*., 2000), it is reasonable to speculate that some chlorophyll *b*-binding sites accept chlorophyll *a* in the same orientation. Hereby, in both PSI and PSII systems the minimal photosystem structure is maintained but the aggregation between single units, triggered by antenna proteins, is lost.

Lhcb monomerization could be elicited by the simultaneous decrease of xanthophylls during the first 10 d of iron deficiency in spinach leaves. In fact, after 13 d of iron deficiency, when both violaxanthin and zeaxanthin xanthophylls increased again, a *de novo* formation of Lhcb trimers and Lhca dimers was observed. Recent studies have indicated that Lhcs have the flexibility to bind not only chlorophylls, but also different carotenoid molecules (Ruban *et al*., 2002). Interestingly, in the *aba1 Arabidopsis* mutant, violaxanthin and neoxanthin are replaced by zeaxanthin, and the Lhcbs are mainly in their monomeric forms (Tardy and Havaux, 1996; Lokstein *et al*., 2002). Moreover, in the *Arabidopsis lut2 npq2* double mutant, all xanthophylls are replaced constitutively by zeaxanthin, and the major antenna, Lhcb, does not form trimers (Havaux *et al*., 2004). Addition of iron to iron-deficient plants re-activated chlorophyll synthesis, but both antheraxanthin and zeaxanthin are strongly reduced, supporting the hypothesis that decreases in chlorophylls are paralleled by zeaxanthin production. Thus, the

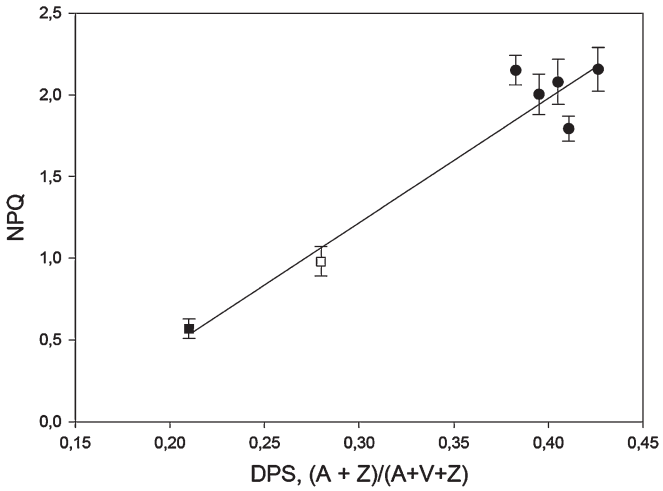

Fig. 9. The relationship between the non-photochemical quenching of fluorescence estimating the light dissipated non-radiatively and calculated on the basis of the ratio between maximal fluorescence in the dark and in the light [NPQ= $(F_m/F'_m)-^1$], and the de-epoxidation status of xanthophylls (the amount of antheraxanthin+zeaxanthin divided by the sum of antheraxanthin+zeaxanthin+violaxanthin=DPS). The relationship is shown for leaves before iron deficiency (filled square), after 13–18 d of iron deficiency (filled circles, each circle representing samples taken on a single day), and 7 d after re-supplying iron (open square). Fluorescence data were replicated on four different leaves per single data point, and means ±SE are shown. The regression line shows that the parameters are tightly associated (r^2=0.92).

observed change in the monomer–trimer equilibrium of major PSII antenna is possibly the result of xanthophyll and chlorophyll fluctuations as an adaptation strategy to iron deficiency in higher plants, playing a role in the energy dissipation mechanisms, as here also assessed by changes in the non-photochemical quenching of fluorescence (see below). The observed loss of superorganization, such as trimerization and dimerization, of antenna proteins was also observed in *Rhodella violocea* upon iron deficiency (Doan *et al*., 2003). Non-denaturating PAGE separation of the chlorophyll–protein complexes indicated that the monomeric form of PSI is also favoured over the trimeric form of PSI under iron stress in cyanobacteria (Ivanov *et al*., 2006), which suggests that changing the aggregation state could represent a common strategy in both higher plants and smaller organisms.

Electron microscopy shows disorganization of chloroplast structure in iron-deficient leaves

Electron micrographs from iron-deficient plants revealed plastids with a strong reduction in thylakoid bending, few photosynthetic lamellae, and with some rudimentary grana. These classical features of thylakoid disorganization induced by iron deprivation have been described previously (Platt-Aloia *et al*., 1983). In the iron-deficient spinach leaves examined here, digitonin cleavage showed that stromal lamellae harboured significant amounts of PSII components, indicating an altered distribution pattern for the reduced PSI and PSII complexes. Good connectivity between photosystems is essential for efficient photosynthesis, and, since the kinetics of the trapping of excitation energy are much faster in PSI than in PSII, in iron-deficient leaves the loss of physical separation between PSI and PSII might have led to an uncontrolled flow of energy from PSII to PSI (Trissl and Wilhelm, 1993). This might also have been the reason why a very large non-photochemical quenching of fluorescence, associated with the activation of light dissipation mechanisms, was observed in iron-deficient leaves (Larbi *et al*., 2006) and could not be fully recovered after a few days of iron nutrition in the present experiment. In cyanobacteria, the physiological consequences of the anatomical alterations observed upon iron deficiency are a reduction of linear electron transport activity through PSII, an increase of cyclic electron flow around PSI, and an increase in respiratory activity (Michel and Pistorius, 2004). The increase in cyclic electron flow around PSI under iron limitation is a consequence of the formation of the PSI–IsiA supercomplex (Michel *et al*., 2003). Cyanobacteria may also utilize a PSII-like protein as an extra antenna for PSI, which shows the flexibility of cyanobacterial light-harvesting systems, and may be a valuable strategy to compensate for the reduction of phycobilisome and PSI levels in response to iron deficiency (Melkozernov *et al*., 2006).

Photosynthetic efficiency of light use is reduced and non-photochemical dissipation of light is increased in iron-deficient leaves

It was also a matter of investigation whether changes in the structure of photosystems of iron-deficient leaves would adversely affect photosynthesis. As expected, photosynthesis was dramatically inhibited at the same time point at which chloroplast ultrastructure and protein composition were observed to be affected by iron deficiency. Photosynthesis was also rather low in control leaves with respect to rates usually found in spinach (Delfine *et al*., 1999), which may be attributed to the hydroponic nutrition of the samples. However, differences between controls and iron-deficient leaves were highly significant. The reduced assembly of PSII into supercomplexes and the macro-organization of supercomplexes in the thylakoid membrane probably determined the large drop in the apparent quantum efficiency of PSII. Iron-deficient leaves were less efficient at using light when this was limiting, as shown by the different slope of the linear response of photosynthesis at increasing, but dim light intensities. Interestingly, however, photosynthesis was also largely inhibited under saturating light intensity, showing that light use is impaired irrespective of the received light, and suggesting that photosynthesis may actually be even more damaged when iron-deficient plants are exposed to bright light. It should also be noted that this reduction of photosynthesis under both low and saturating light intensity was only partially recovered 7 d after restoring iron nutrition. A strong reduction in the Rubisco protein in the thylakoids of iron-deficient leaves was observed (Fig. 3B). This is in agreement with previous investigations which found that the initial physiological response to iron deficiency in sugar beet leaves appears to be loss of both photochemical and biochemical (i.e. CO_2 fixation by RuBP carboxylase) capacities of CO_2 assimilation. The lower RuBP carboxylation capacity was not previously attributed to reduced activation of the Rubisco enzyme (Taylor and Terry, 1984), but rather to a down-regulation of gene expression, resulting in RuBP levels reduced by ~70%. Biochemical damage leading to a reduction in CO_2 capture by Rubisco may therefore also play a role in inhibiting photosynthesis of iron-deficient leaves, even when light is not a limiting factor.

Chlorophyll fluorescence analysis is usually an excellent tool to study *in vivo* photochemical damage. Morales *et al*. (2001), however, pointed out that the maximal yield of fluorescence in dark-adapted leaves (F_v/F_m) may not indicate real damage of PSII in iron-deficient leaves. These authors demonstrated that iron deficiency may also disconnect PSII antennae from reaction centres, and that fluorescence may also be released from disconnected PSII antennae. However, both the quantum yield of photosynthesis and the fluorescence maximal yield of dark-adapted

leaves were strongly reduced by the present treatment. This is interpreted as an independent indication of PSII photoinhibition, which does not necessarily involve mechanisms leading to underestimation of F_v/F_m.

The fluorescence quenching also indicated a substantial reduction in photochemical electron transport and the activation of energy dissipation mechanisms in light-adapted, iron-deficient leaves. The increase of non-photochemical quenching due to iron deficiency reflected the de-epoxidation of xanthophylls and the thermal dissipation in the photosystem antennae (Brugnoli *et al*., 1998), as also previously observed in iron-deficient leaves (Larbi *et al*., 2004). The two parameters were also associated in leaves recovering from iron deficiency, again confirming previous observations that zeaxanthin may be re-converted to violaxanthin if iron becomes available, and that this reveals a reduced thermal dissipation in PSII antennae (Larbi *et al*., 2004). Larbi *et al*. (2004) observed that re-conversion of xanthophylls was fast but incomplete, occurring just 2 d after supplying iron. This experiment was extended to show that, even 7 d after iron is restored, the de-epoxidation status does not reach the low value of non-stressed leaves, and a still considerable fraction of energy is therefore dissipated thermally, which is consistent with the observed incomplete recovery of photosynthesis in the same leaves. The de-epoxidation status of xanthophylls also changed (decreased) to a relevant extent between 13 d and 18 d of iron deficiency, when violaxanthin surprisingly recovered from its minimum. This was not reflected in a concurrent change of the non-photochemical quenching. This result is interpreted as indicating that there are changes in xanthophyll de-epoxidation during iron deficiency that are not linked to dissipation mechanisms. However, it is also possible that the non-photochemical quenching parameter is not sensitive enough as an indicator of thermal dissipation, as revealed by xanthophyll de-epoxidation.

Conclusions

Iron deficiency induced immediately after germination causes heavy damage to the photochemical apparatus of spinach, which is not recoverable after a few days of regular iron nutrition. Cyanobacteria, growing photoautotrophically, have evolved mechanisms to modify and/or protect their chlorophyll protein complexes. The photosynthetic apparatus of these lower organisms is under constant change to adapt to the environment and to the daily alterations. This does not seem to be the case in higher plants in which no expression of new proteins is observed and no specific protein is missing in iron-deficient conditions. Iron deficiency rapidly induces a total reduction of the pigments and proteins of the photosynthetic apparatus, mirrored by a reduction of the photosynthetic rate, a specific reduction of PSII antennae, the disappearance of supercomplexes followed by re-arrangements as a consequence of an altered aggregation of the monomer–trimer equilibrium of the major PSII antennae, and the reduction of xanthophylls. The recovery of xanthophylls after a few days of stress is not matched by a reduction of the non-photochemical dissipation of light energy in the present analysis of fluorescence, but may play a role in the rearrangement of the PSII structure and may constitute a first adaptive adjustment of the photochemical apparatus to cope with iron deficiency.

Acknowledgements

We gratefully acknowledge Dr Anna Rita Taddei (Università della Tuscia, Viterbo) for providing the electron microscope photographs. We would like to thank Dr Jaqueline Scarpa for manuscript revision. This work was financially supported by grants from the Italian Ministry for University Research (MIUR-PRIN 2004).

References

Andaluz S, Millan AF, De las Rivas J, Aro EM, Abadìa J, Abadìa A. 2006. Proteomic profiles of thylakoid membranes and changes in response to iron deficiency. *Photosynthesis Research* **89,** 141–155.

Aro EM, Suorsa M, Rokka A, Allahverdiveva Y, Paakkarinen V, Saleem A, Battchikova N, Rintamaki E. 2005. Dynamics of photosystem II: a proteomic approach to thylakoid protein complexes. *Journal of Experimental Botany* **56,** 347–356.

Bassi R, Croce R, Cugini D, Sandona D. 1999. Mutational analysis of a higher plant antenna protein provides identification of chromophores bound into multiple sites. *Proceedings of the National Academy Sciences, USA* **96,** 10056–10061.

Bibby TS, Nield J, Barber J. 2001. Iron deficiency induces the formation of an antenna ring around trimeric photosystem I in cyanobacteria. *Nature* **412,** 743–745.

Bilger W, Bjorkman O. 1994. Relationship among violaxanthin deepoxidation, thylakoid membrane conformation, and non-photochemical chlorophyll fluorescence quenching in leaves of cotton (*Gossypium hirsutum* L.). *Planta* **193,** 238–246.

Boekema EJ, Hifney A, Yakushevska AE, Piotrowski M, Keegstra W, Berry S, Michel KP, Pistorius EK, Kruip J. 2001. A giant chlorophyll–protein complex induced by iron deficiency in cyanobacteria. *Nature* **412,** 745–748.

Brugnoli E, Scartazza A, De Tullio MC, Monteverdi MC, Lauteri M, Augusti A. 1998. Zeaxanthin and non-photochemical quenching in sun and shade leaves of C-3 and C-4 plants. *Physiologia Plantarum* **104,** 727–734.

Candiano G, Bruschi M, Musante L, Cantucci L, Ghiggeri GM, Carnemolla B, Orecchia P, Zardi L, Righetti PG. 2004. Blue silver: a very sensitive colloidal Coomassie G-250 staining for proteome analysis. *Electrophoresis* **25,** 1327–1333.

Caffari S, Croce R, Cattivelli L, Bassi R. 2004. A look within LHCB: differential analysis of the Lhcb1–3 complexes building the major trimeric antenna complex of higher-plant photosynthesis. *Biochemistry* **43,** 9467–9476.

Chen M, Bibby TS, Nield J, Larkuma A, Barber J. 2005. Iron deficiency induces a chlorophyll d-binding Pcb antenna system around photosystem I in *Acaryochloris marina*. *Biochimica et Biophysica Acta* **1708,** 367–374.

Ciambella C, Roepstorff P, Aro EM, Zolla L. 2005. A proteomic approach for investigation of photosynthetic apparatus in plants. *Proteomics* **5,** 746–757.

Croce R, Zucchelli G, Garlaschi FM, Jennings RC. 1998. Thermal broadening study of the antenna chlorophylls in PSI-200, LHCI, and PSI core. *Biochemistry* **37,** 17355–17360.

De las Rivas J, Abadìa A, Abadìa J. 1989. A new reversed phase-HPLC method resolving all major higher plant photosynthetic pigments. *Plant Physiology* **91,** 190–192.

Dekker JP, Boekema EJ. 2005. Supramolecular organization of thylakoid membrane proteins in green plants. *Biochimica et Biophysica Acta* **1706,** 12–39.

Delfine S, Alvino A, Villani MC, Loreto F. 1999. Restrictions to CO_2 conductance and photosynthesis in spinach leaves recovering from salt stress. *Plant Physiology* **119,** 1101–1106.

Demmig B, Winter K, Krüger A, Czygan F-C. 1987. Photoinhibition and zeaxanthin formation in intact leaves: a possible role of the xanthophyll cycle in the dissipation of excess light energy. *Plant Physiology* **84,** 218–224.

Doan JM, Schoefs B, Ruban AV, Etienne AE. 2003. Changes in the LHCI aggregation state during iron repletion in the unicellular red alga *Rhodella violacea*. *FEBS Letters* **533,** 59–62.

Dudley JW. 1958. Number of chloroplasts in the guard cells of inbred lines of tetraploid and diploid sugar beets. *Agronomy Journal* **50,** 169–170.

Espen L, Dell'Orto M, De Nisi P, Zocchi G. 2000. Metabolic responses in cucumber (*Cucumis sativus* L.) roots under Fe-deficiency: a 31P-nuclear magnetic resonance in-vivo study. *Planta* **210,** 985–992.

Genty B, Briantais J-M, Baker NR. 1989. The relationship between the quantum yield of photosynthetic electron transport and quenching of chlorophyll fluorescence. *Biochimica et Biophysica Acta* **990,** 87–92.

Gilmore AM, Yamamoto HY. 1992. Dark induction of zeaxanthin-dependent nonphotochemical fluorescence quenching mediated by ATP. *Proceedings of the National Academy Sciences, USA* **89,** 1899–1903.

Gomez SM, Nishio JN, Faull KF, Whitelegge JP. 2002. The chloroplast grana proteome defined by intact mass measurements from liquid chromatography mass spectrometry. *Molecular and Cellular Proteomics* **1,** 46–59.

Goodenough UW, Levine RP. 1969. Chloroplast ultrastructure in mutant strains of *Chlamydomonas reinhardi* lacking components of the photosynthetic apparatus. *Plant Physiology* **44,** 990–1000.

Granvogl B, Reisinger V, Eichacker LA. 2006. Mapping the proteome of thylakoid membranes by *de novo* sequencing of intermembrane peptide domains. *Proteomics* **6,** 3681–3695.

Guikema JA, Sherman LA. 1983. Chlorophyll–protein organization of membranes from the cyanobacterium *Anacystis nidulans*. *Archives of Biochemistry and Biophysics* **220,** 155–166.

Havaux M, Dall'Osto L, Cuine S, Giuliano G, Bassi R. 2004. The effect of zeaxanthin as the only xanthophyll on the structure and function of the photosynthetic apparatus in *Arabidopsis thaliana*. *Journal of Biological Chemistry* **279,** 13878–13888.

Hippler M, Klein J, Fink A, Allinger T, Hearth P. 2001. Towards functional proteomics of membrane protein complexes: analysis of thylakoid membranes from *Chlamydomonas reinhardtii*. *The Plant Journal* **28,** 595–606.

Hou CX, Dirk LMA, Williams MA. 2004. Inhibition of peptide deformylase in *Nicotiana tabacum* leads to decreased d1 protein accumulation, ultimately resulting in a reduction of photosystem II complexes. *American Journal of Botany* **91,** 1304–1311.

Huber CG, Walcher W, Timperio AM, Troiani S, Porceddu A, Zolla L. 2004. Multidimensional proteomic analysis of photosynthetic membrane proteins by liquid extraction–ultracentrifugation–liquid chromatography–mass spectrometry. *Proteomics* **4,** 3909–3920.

Ivanov AG, Krol M, Sveshnikov D, *et al*. 2006. Iron deficiency in cyanobacteria causes monomerization of photosystem I trimers and reduces the capacity for state transitions and the effective absorption cross section of photosystem I *in vivo*. *Plant Physiology* **141,** 1436–1445.

Johnson G, Scholes JD, Horton P, Young AJ. 1993. Relationships between carotenoid composition and growth habit in British plant species. *Plant, Cell and Environment* **16,** 681–686.

Kűgler MJ, Lothar KV, Schmitz UK, Braun HP. 1997. Analysis of the chloroplast protein complexes by blue-native polyacrylamide gel electrophoresis (BN-PAGE). *Photosynthesis Research* **53,** 35–44.

Laemmli UK. 1970. Cleavage of structural proteins during the assembly of the head of bacteriophage T4. *Nature* **227,** 680–686.

Larbi A, Abadìa A, Javier A, Morales F. 2006. Down co-regulation of light absorption, photochemistry, and carboxylation in Fe-deficient plants growing in different environments. *Photosynthesis Research* **89,** 113–126.

Larbi A, Abadìa A, Morales F, Abdia J. 2004. Fe resupply to Fe-deficient sugar beet plants leads to rapid changes in the violaxanthin cycle and other photosynthetic characteristics without significant *de novo* chlorophyll synthesis. *Photosynthesis Research* **79,** 59–69.

Lax JEM, Arteni AA, Boekema EJ, Pistorius EK, Michel KP, Rögner M. 2007. Structural response of photosystem 2 to iron deficiency: characterization of a new photosystem 2–IdiA complex from the cyanobacterium *Thermosynechococcus elongatus* BP-1. *Biochimica et Biophysica Acta* **1767,** 528–534.

Lokstein H, Tian L, Polle JEW, Della Penna D. 2002. Xanthophyll biosynthetic mutants of *Arabidopsis thaliana*: altered nonphotochemical quenching of chlorophyll fluorescence is due to changes in photosystem II antenna size and stability. *Biochimica et Biophysica Acta* **1553,** 309–319.

Loll B, Kern J, Saenger W, Zouni A, Biesiadka J. 2005. Towards complete cofactor arrangement in the 3.0 Å resolution structure of photosystem II. *Nature* **438,** 1040–1044.

Loreto F, Harley PC, Di Marco G, Sharkey TD. 1992. Estimation of mesophyll conductance to CO_2 flux by three different methods. *Plant Physiology* **98,** 1437–1443.

Melkozernov AN, Barber J, Blankenship RE. 2006. Light harvesting in photosystem I supercomplexes. *Biochemistry* **45,** 331–345.

Michel KP, Berry S, Hifney A, Pistorius EK. 2003. Adaptation to iron deficiency: a comparison between the cyanobacterium *Synechococcus elongatus* PCC 7942 wild-type and a DpsA-free mutant. *Photosynthesis Research* **75,** 71–84.

Michel KP, Pistorius EK. 2004. Adaptation of the photosynthetic electron transport chain in cyanobacteria to iron deficiency: the function of IdiA and IsiA. *Physiologia Plantarum* **120,** 36–50.

Morales F, Grasa R, Abadìa A, Abadìa J. 1998. Iron chlorosis paradox in fruit trees. *Journal of Plant Nutrition* **21,** 815–825.

Morales F, Moise N, Quilez R, Abadìa A, Abadìa J, Moya I. 2001. Iron deficiency interrupts energy transfer from a disconnected part of the antenna to the rest of photosystem II. *Photosynthesis Research* **70,** 207–220.

Moseley JL, Allinger T, Herzog S, Hoerth P, Wehinger E, Merchant S, Hippler M. 2002. Adaptation to Fe-deficiency requires remodeling of the photosynthetic apparatus. *EMBO Journal* **21,** 6709–6720.

Naumann B, Stauber EJ, Busch A, Sommer F, Hippler M. 2005. N-terminal processing of Lhca3 is a key step in

remodelling of the photosystem I-light-harvesting complex under iron deficiency in *Chlamydomonas reinhardtii*. *Journal of Bioogical Chemistry* **280,** 20431–20441.

Nishio JN. 1985. *Iron nutrition-mediated chloroplast development*. University of California, Berkeley, CA, USA. Avail Univ. Microfilms Int. 104 pp.

Nisi PD, Zocchi G. 2000. Phosphoenolpyruvate carboxylase in cucumber (*Cucumis sativus* L.) roots under iron deficiency: activity and kinetic characterization. *Journal of Experimental Botany* **51,** 1903–1909.

Nishimura M, Graham D, Akazawa T. 1976. Isolation of intact chloroplasts and other cell organelles from spinach leaf protoplasts. *Plant Physiology* **58,** 309–314.

Pakrasi HB, Riethman HC, Sherman LA. 1985. Organization of pigment proteins in the photosystem II complex of the cyanobacterium *Anacystis nidulans* R2. *Proceedings of the National Academy Sciences, USA* **82,** 6903–6907.

Pattanayak GK, Biswala AK, Reddyb VS, Tripathya BC. 2005. Light-dependent regulation of chlorophyll b biosynthesis in chlorophyllide a oxygenase overexpressing tobacco plants. *Biochemical and Biophysical Research Communications* **326,** 466–471.

Platt-Aloia KA, Thomson WW, Terry N. 1983. Changes in plastid ultrastructure during iron nutrition-mediated chloroplast development. *Plant Physiology* **78,** 269–299.

Polle JEW, Benemann JR, Tanaka A, Melis A. 2000. Photosynthetic apparatus organization and function in the wild type and a chlorophyll b-less mutant of *Chlamydomonas reinhardtii*: dependence on carbon source. *Planta* **211,** 335–344.

Ruban AV, Pascal A, Lee PJ, Robert B, Horton P. 2002. Molecular configuration of xanthophyll cycle carotenoids in photosystem II antenna complexes. *Journal of Biological Chemistry* **277,** 42937–42942.

Sandstrom S, Ivanov AG, Park YI, Oquist G, Gustafsson P. 2002. Iron stress responses in the cyanobacterium *Synechococcus* sp. PCC 7942. *Physiologia Plantarum* **116,** 255–263.

Spiller S, Terry N. 1980. Limiting factors in photosynthesis.II. Iron stress diminishes photochemical capacity by reducing the number of photosynthetic units. *Plant Physiology* **65,** 121–125.

Straus NA. 1994. Iron deprivation: physiology and gene regulation. In: Bryant DA, ed. *The molecular biology of cyanobacteria*. Dordrecht, The Netherlands: Kluwer, 731–750.

Suorsa M, Regel RE, Paakkarinen V, Battchikova N, Herrmann RG, Aro EM. 2004. Protein assembly of photosystem II and accumulation of subcomplexes in the absence of low molecular mass subunits PsbL and PsbJ. *European Journal of Biochemistry* **271,** 96–107.

Susín S, Abián J, Peleato ML, Sánchez-Baeza J, Abadía A, Gelpí E, Abadía J. 1994. Flavin excretion from iron deficient sugar beet (*Beta vulgaris* L.). *Planta* **193,** 514–519.

Tanaka R, Koshino Y, Sawa S, Sumie Ishiguro S, Okada K, Tanaka A. 2001. Overexpression of chlorophyllide a oxygenase (CAO) enlarges the antenna size of photosystem II in *Arabidopsis thaliana*. *The Plant Journal* **26,** 365–373.

Tanaka R, Tanaka A. 2005. Effects of chlorophyllide a oxygenase overexpression on light acclimation in *Arabidopsis thaliana*. *Photosynthesis Research* **85,** 327–340.

Tardy F, Havaux M. 1996. Photosynthesis, chlorophyll fluorescence, light-harvesting system and photoinhibition resistance of a zeaxanthin-accumulating mutant of *Arabidopsis thaliana*. *Journal of Photochemistry and Photobiology B* **34,** 87–94.

Taylor SE, Terry N. 1984. Limiting factors in photosynthesis: V. Photochemical energy supply colimits photosynthesis at low values of intercellular CO_2 concentration. *Plant Physiology* **75,** 82–86.

Thoiron S, Pascal N, Briat JF. 1997. Impact of iron deficiency and iron re-supply during the early stages of vegetative development in maize (*Zea mays* L.). *Plant, Cell and Environment* **20,** 1051–1060.

Timperio AM, Huber CG, Zolla L. 2004. Separation and identification of the light harvesting proteins contained in grana and stroma thylakoid membrane fractions. *Journal of Chromatography A* **1040,** 73–81.

Trissl HW, Wilhelm C. 1993. Why do thylakoid membranes from higher plants form grana stacks? *Trends in Biochemical Sciences* **18,** 415–419.

Val J, Abadìa J, Heras L, Monge E. 1986. Higher plant photosynthetic pigment analysis. Determination of carotenoids and chlorophylls by HPLC. *Journal of Micronutrition Analysis* **2,** 305–312.

Van Kooten O, Snel JFH. 1990. The use of chlorophyll fluorescence nomenclature in plant stress physiology. *Photosynthesis Research* **25,** 147–150.

Whitelegge JP, Laganowsky A, Nishio J, Souda P, Zhang H, Cramer WA. 2006. Sequencing covalent modifications of membrane proteins. *Journal of Experimental Botany* **57,** 1515–1522.

Xu H, Vavilin D, Vermaas W. 2001. Chlorophyll b can serve as the major pigment in functional photosystem II complexes of cyanobacteria. *Proceedings of the National Academy Sciences, USA* **98,** 14168–14173.

Zolla L, Rinalducci S, Timperio AM. 2007. Proteomic analysis of photosystem I components from different plant species. *Proteomics* **7,** 1866–1876.

Zolla L, Rinalducci S, Timperio AM, Huber CG. 2002. Proteomics of light-harvesting proteins in different plant species: analysis and comparison by liquid chromatography-electrospray ionization mass spectrometry. Photosystem I. *Plant Physiology* **130,** 1938–1950.

Zolla L, Rinalducci S, Timperio AM, Huber CG, Righetti PG. 2004. Intact mass measurements for unequivocal identification of hydrophobic photosynthetic photosystems I and II antenna proteins. *Electrophoresis* **25,** 1353–1366.

Zolla L, Timperio AM, Walcher W, Huber CG. 2003. Proteomics of light-harvesting proteins in different plant species: analysis and comparison by liquid chromatography-electrospray ionization mass spectrometry. Photosystem II. *Plant Physiology* **131,** 198–214.